

# Effect of the Dynamic Resistance on the Maximum Output Power in Dynamic Modelling of Photovoltaic Solar Cells

Siaka Touré

Solar Energy Laboratory, Félix Houphouët-Boigny University of Abidjan Cocody, Abidjan, Côte d'Ivoire

Email: siakahtoure@yahoo.fr

**How to cite this paper:** Touré, S. (2022) Effect of the Dynamic Resistance on the Maximum Output Power in Dynamic Modelling of Photovoltaic Solar Cells. *Open Journal of Modelling and Simulation*, 10, 48-57. <https://doi.org/10.4236/ojmsi.2022.101003>

**Received:** August 9, 2021

**Accepted:** December 14, 2021

**Published:** December 17, 2021

Copyright © 2022 by author(s) and Scientific Research Publishing Inc. This work is licensed under the Creative Commons Attribution International License (CC BY 4.0).

<http://creativecommons.org/licenses/by/4.0/>



Open Access

## Abstract

Several studies on PV solar cells are found in the literature which use static models. Those models are mainly one-diode, two-diode or three-diode models. In the dynamic modelling, a variable parallel capacitance is incorporated. Unlike the previous studies which do not clearly establish a relationship between the capacitance and the voltage, in the present paper, the link between the capacitance and the voltage is investigated and established. In dynamic modelling investigated in this paper, the dynamic resistance is introduced in the modelling of the solar cell. It is introduced in the current-voltage characteristic. The value of the dynamic resistance is evaluated at the maximum power point and its effect on the maximum power is investigated. The study shows for the first time, that the dynamic resistance must be introduced in the current-voltage characteristic, because it has an influence on the PV cell output.

## Keywords

Photovoltaic Solar Cells, Dynamic Modelling, Dynamic Resistance, Diffusion Capacitance, Transition Capacitance

## 1. Introduction

The world is facing an energy crisis due to the growing energy demand and the environmental damages linked to fossil fuel energy sources. Photovoltaic conversion of solar energy is an alternative source which is clean, sustainable and very promising, because of the researches for higher efficiency solar cells. Several PV models have been studied. Most of them are static models based on a single

diode and some parasitic parameters [1] [2] [3]. Other simulations are based on a two-diode model [4] [5] [6] [7]. The one-diode, two-diode and three-diode models have also been used in several works on hybrid Photovoltaic/Thermal panels [8] [9]. Comparatively to the works about the static models, few studies are made about dynamic modelling. The dynamic modelling incorporates a variable parallel capacitance. The different parameters of those models, such as the PV cell impedance, are frequency dependant. In [10], the effect of capacitance on the output characteristics of solar cells is discussed. The model takes the parallel capacitance and the parasite resistances  $R_{sh}$  and  $R_s$  into account. The I - V curves are drawn for different frequencies. A split of the characteristics is observed, which is due to the charge or discharge of the internal capacitance. The model is built in a MATLAB environment. In [11], the dynamic model also includes a parallel capacitance as well as  $R_{sh}$  and  $R_s$ . The bases of the Impedance Spectroscopy (IS) are explained and applied to detect the Potential-Induced Degradation (PID) of c-Si PV panels. In [12], a dynamic PV model is studied, which incorporates capacitance and reverse-bias characteristics. The model also includes a series inductance. Some cell parameters are obtained from measurements of the impedance at various frequencies. The nonlinear equation of the I - V characteristics is numerically solved using MATLAB Simulink Toolbox. Some work has also been made to study the effect of solar array capacitance on the performance of switching shunt voltage regulator [13]. Some other work has been performed for the characterization of solar cells by Impedance Spectroscopy [14]. The dynamic modelling is also a tool for the study of Negative Capacitance (NC) that has some effects in Organic Light-Emitting Diodes (OLEDs) [15] [16] [17]. This literature review shows that, in the case of dynamic modelling of the PV cell, the parallel capacitance is a very important parameter. But the previous studies do not clearly establish a relationship between the capacitance and the voltage; moreover, in those previous dynamic modellings, where the capacitance effect is investigated, the dynamic resistance is not included in the I - V characteristic. In the present paper, a clear relationship between the capacitance and the voltage is investigated. Moreover, the dynamic resistance  $R_d$  is introduced in the current-voltage characteristic, which leads to a new expression of this current-voltage characteristic. The value of  $R_d$  is evaluated at the maximum power point in order to know whether it has an effect or not on the maximum output power of the PV cell.

## 2. Method

The capacitance and its variation with time as well as the voltage have an importance effect on the dynamic behaviour of a PV cell. Hence, the investigation undertaken in this paper will, in a first time, focus on the capacitance, to have a clear relation of its variation with the voltage. Then, in a second step, the dynamic resistance will be introduced in the dynamic model of the solar cell, leading to its introduction in the current-voltage characteristic.

## 2.1. The Capacitance of the Solar Cell

A variation of the voltage applied to a p-n junction is linked to a variation of charge, which yields a capacitance. Two different capacitances have to be taken into account: the transition (or space charge) capacitance  $C_t$  and the diffusion capacitance  $C_d$ .  $C_d$  and  $C_t$  are parallel, so that the cell capacitance is expressed as:

$$C = C_d + C_t \quad (1)$$

In dynamic regime, the junction schematic representation is given in **Figure 1**.

Therefore, the effect of the transition and diffusion capacitance on the diode is sketched in **Figure 2**.

In several papers [12] [18], the junction or transition capacitance, which is due to the charges stored in the depletion region, is expressed as:

$$C_t = \frac{C_0}{\sqrt{1 - \frac{V_d}{\Phi}}} \quad (2)$$

In Equation (2),  $\Phi$  is the diffusion potential;  $V_d = U$  is the voltage over the diode;  $C_0$  is the voltage for  $U = 0$ . The voltage  $V = \Phi - U$  is the potential between the limits of the depletion region. The transition capacitance dominates for small voltages.

The diffusion capacitance  $C_d$  is due to the charges stored outside the depletion region, in the neutral regions, when the solar cell is under illumination. In some works [12], it is expressed as:

$$C_d = \frac{\tau I_d}{nV_T} \quad (3)$$

In Equation (3),  $\tau$  is the mean carrier lifetime.  $I_d$  is the current conducted by the forward biased diode.  $V_T$  is the thermal voltage and is expressed as:

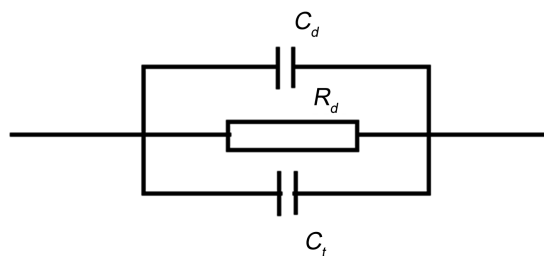


**Figure 1.** Schematic representation of the junction in dynamic regime.

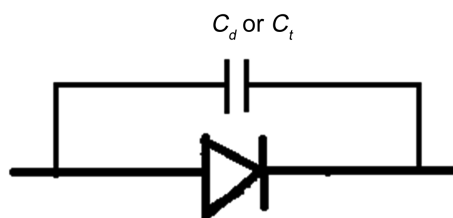


**Figure 2.** Effect of the transition and diffusion capacitances on the diode.

$$V_T = \frac{KT}{q} \quad (4)$$

$C_d$  dominates for forward biased p-n junctions.

In several works, the Negative Capacitance (NC) is studied. The admittance  $Y(\omega)$ , for a frequency  $\omega$ , is expressed as [15]:

$$Y(\omega) = \frac{\delta I(\omega)}{\delta V(\omega)} \quad (5)$$

for  $\delta I$  and  $\delta V \sim e^{i\omega t}$ .

A small  $\delta V$  voltage impulse yields a transient harmonic current  $\delta I$ . The capacitance is expressed as:

$$C(\omega) = \frac{1}{\omega} \text{Im}[Y(\omega)] \quad (6)$$

The conductance  $g(\omega)$  is expressed as:

$$g(\omega) = \text{Re}[Y(\omega)] \quad (7)$$

In all cases, the capacitance is linked to the voltage. In several works [19] [20], the capacitance is linked to the excess minority carrier's density under illumination. Let a p-n junction under illumination be considered. In the p base, the excess minority carriers density generated  $\delta(x)$  is gotten from the continuity equation. The resolution of this equation yields the photocurrent density  $J_{ph}$ , the photovoltage  $V_{ph}$  and the capacitance. The photovoltage  $V_{ph}$  is expressed as:

$$V_{ph} = V_T \ln \left[ 1 + \frac{N_b \delta(0)}{n_i^2} \right] \quad (8)$$

where  $\delta(0) = \delta(x=0)$ ;  $N_b$  is the base doping density;  $n_i$  is the intrinsic carriers density. The transition capacitance  $C_t$  and the diffusion capacitance  $C_d$  are expressed as [19] [20]:

$$C_t = \frac{q}{V_T} \frac{n_i^2}{N_b} \quad (9)$$

$$C_d = \frac{q}{V_T} \delta(0) \quad (10)$$

Hence, from Equation (1), one gets:

$$C = \frac{q}{V_T} \frac{n_i^2}{N_b} + \frac{q}{V_T} \delta(0) \quad (11)$$

Moreover, from Equation (8), for  $V = V_{ph}$  one gets:

$$1 + \frac{N_b \delta(0)}{n_i^2} = e^{\frac{V}{V_T}} \quad (12)$$

Consequently, one gets:

$$\delta(0) = \frac{n_i^2}{N_b} \left( e^{\frac{V}{V_T}} - 1 \right) \quad (13)$$

Then the capacitance, given by Equation (11), becomes:

$$C = \frac{q}{V_T} \frac{n_i^2}{N_b} + \frac{q}{V_T} \frac{n_i^2}{N_b} \left( e^{\frac{V}{V_T}} - 1 \right) \tag{14}$$

Finally, one gets:

$$C = \frac{q}{V_T} \frac{n_i^2}{N_b} e^{\frac{V}{V_T}} \tag{15}$$

Equation (15) shows explicitly, for the first time, the voltage dependence of the capacitance.

### 2.2. Dynamic Model and Dynamic Resistance Estimate

Very often, the single diode dynamic model is used for the dynamic study of solar cells. In some of the studies, only the forward-bias conducting diode  $D_f$ , the parallel capacitance  $C_p$  (which is voltage dependant), the shunt resistance  $R_{sh}$  and the series resistance  $R_s$ , are taken into account, as shown in **Figure 3** [10] [11].

In such model, the impedance  $Z$  of the circuit is given by:

$$Z = \text{Re}(Z) + j \text{Im}(Z) \tag{16}$$

where:

$$\text{Re}(Z) = R_s + \frac{R_{sh}}{1 + \omega^2 C_p^2 R_{sh}^2} \tag{17}$$

$$\text{Im}(Z) = -\frac{\omega C_p R_{sh}^2}{1 + \omega^2 C_p^2 R_{sh}^2} \tag{18}$$

In Equations (17) and (18),  $\omega$  is the frequency. In other works [12], a more extended model is used, which, in addition, includes a series inductance  $L_s$  and a reverse-bias diode  $D_r$ , with a breakdown voltage  $V_{bd}$  as shown in **Figure 4**.

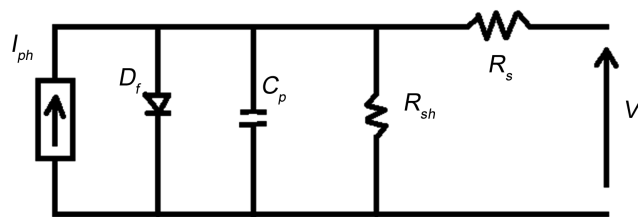


**Figure 3.** Single diode solar cell dynamic model.

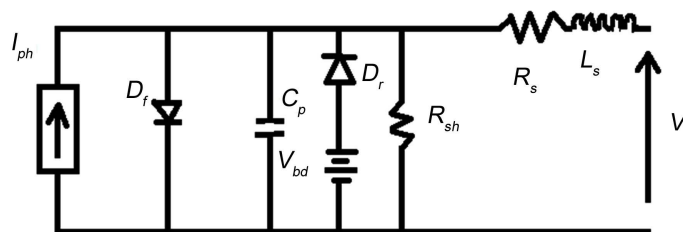


**Figure 4.** PV cell dynamic model including the reverse-bias diode and the series inductance.

For such model, the impedance  $Z$  is expressed as:

$$Z = \left( R_s + \frac{R_{sh}}{\alpha + 1} \right) + j \left( L_s \omega - \frac{\omega C_p R_{sh}^2}{\alpha + 1} \right) \quad (19)$$

where  $\alpha = \omega^2 C_p^2 R_{sh}^2$ .

The study of the variation of  $Z$  with the frequency  $\omega$  is a mean to determine the cell parameters such as  $R_{sh}$ ,  $R_s$ ,  $C_p$  and  $L_s$ .

In the present paper, by taking into account **Figure 1** and **Figure 2**, the dynamic resistance  $R_d$  is included in the model, without the reverse-bias diode and the series inductance, as shown in **Figure 5**.

The introduction of  $R_d$  in the model is justified by the following calculations. Let the capacitance current be considered. The diode voltage  $V_d$  is expressed as:

$$V_d = V + R_s I \quad (20)$$

The charge  $Q$  is:

$$Q = C V_d \quad (21)$$

Therefore, the current  $i$  is given by:

$$i = \frac{\partial Q}{\partial t} = \frac{\partial (C V_d)}{\partial t} = C \frac{\partial V_d}{\partial t} + V_d \frac{\partial C}{\partial t} \quad (22)$$

$$i = C \frac{\partial (V + R_s I)}{\partial t} + (V + R_s I) \frac{\partial C}{\partial t} \quad (23)$$

Then the current-voltage characteristic is given by [10]:

$$I = I_{ph} - I_s \left[ \exp \left( \frac{V + R_s I}{n V_T} \right) - 1 \right] - \frac{V + R_s I}{R_{sh}} - (V + R_s I) \frac{\partial C}{\partial t} - C \frac{\partial (V + R_s I)}{\partial t} \quad (24)$$

In Equation (24),  $I_{ph}$  is the photocurrent,  $I_s$  is the diode saturation current and  $n$  is the diode ideality factor.

In the present paper,  $R_d$  is introduced as indicated below:

For a voltage  $u$  over the capacitance,  $C$  is expressed as:

$$C = \frac{\delta Q}{\delta u} = \frac{\delta i t}{\delta u} = \frac{t}{\frac{\delta u}{\delta i}} \quad (25)$$

Since  $\delta u = R_d \delta i$

One gets:

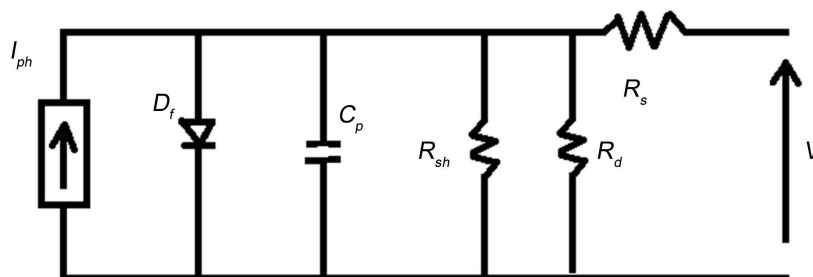


**Figure 5.** Single diode solar cell dynamic model including the dynamic resistance.

$$\frac{\partial C}{\partial t} = \frac{1}{R_d} \quad (26)$$

Moreover:

$$\frac{\partial(V + R_s I)}{\partial t} = \frac{\partial V}{\partial t} + R_s \frac{\partial I}{\partial t} = \frac{\partial V}{\partial t} + R_s \frac{\partial I}{\partial V} \frac{\partial V}{\partial t} = \frac{\partial V}{\partial t} + g R_s \frac{\partial V}{\partial t} \quad (27)$$

In Equation (27),  $g$  is the conductance. Hence:

$$\frac{\partial(V + R_s I)}{\partial t} = \frac{\partial V}{\partial t} (1 + g R_s) \quad (28)$$

Therefore, Equation (24) becomes:

$$I = I_{ph} - I_s \left[ \exp\left(\frac{V + R_s I}{n V_T}\right) - 1 \right] - \frac{V + R_s I}{R_{sh}} - \frac{V + R_s I}{R_d} - C \frac{\partial V}{\partial t} (1 + g R_s) \quad (29)$$

The solution of the nonlinear Equation (29) yields the output of the solar cell under illumination:

If the term  $g R_s \approx 0$ , Equation (29) becomes:

$$I = I_{ph} - I_s \left[ \exp\left(\frac{V + R_s I}{n V_T}\right) - 1 \right] - \frac{V + R_s I}{R_{sh}} - \frac{V + R_s I}{R_d} - C \frac{\partial V}{\partial t} \quad (30)$$

### 3. Results and Discussion

#### 3.1. The Variation of the Capacitance

Let a solar cell be considered with the following parameters:  $V_{oc} = 0.5925$  V ;  $n_i = 1.45 \times 10^{10} \text{ cm}^{-3}$  ;  $N_b = 10^{17} \text{ cm}^{-3}$  ;  $q = 1.602 \times 10^{-19} \text{ C}$  ;  $T = 299.16 \text{ K}$  . A plotting of  $\log C$  against  $V$  is sketched on **Figure 6**. It is a straight line with slope

$a = \frac{1}{\ln 10} \frac{1}{V_T} = 16847$  and intercept  $b = \log C_i = -1.8839$  . For the chosen solar

cell, the voltage increases quickly from 0.013 pF (for the short-circuit) to 125.3  $\mu\text{F}$  (for open voltage  $V_{oc} = 0.5925$  V ).

Hence; for any value of the voltage, the capacitance can be calculated and that is useful for the evaluation of the current as shown by Equation (29) and the impedance.

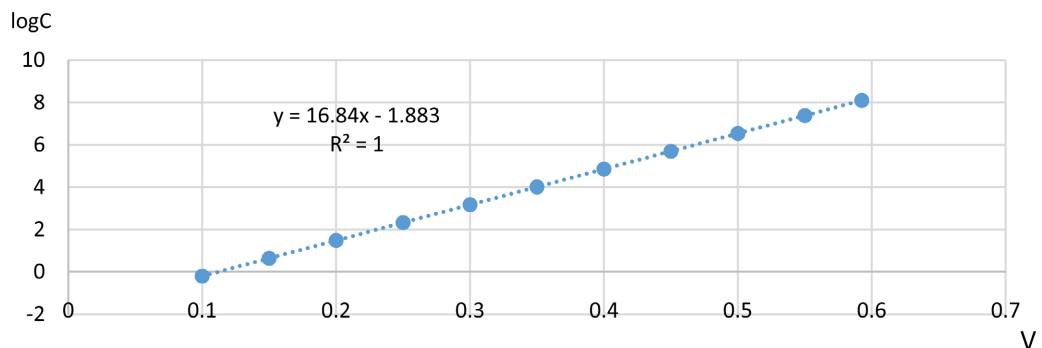


**Figure 6.** Plotting of  $\log C$  against the voltage  $V$ .

### 3.2. Evaluation of the Dynamic Resistance

The evaluation of the dynamic resistance  $R_d$  was made by using the following reduced equation:

$$I = I_{ph} - I_s \left[ \exp\left(\frac{V + R_s I}{nV_T}\right) - 1 \right] - \frac{V + R_s I}{R_{sh}} - \frac{V + R_s I}{R_d} \quad (31)$$

The calculation was made for the following PV cell described in [10]:

$$I_{ph} = 1.035 \text{ A}; \quad I_s = 1.05 \times 10^{-10} \text{ A}; \quad n = 1.2; \quad R_s = 0.08 \text{ } \Omega; \quad R_{sh} = 3.15 \text{ } \Omega$$

At the maximum power point ( $V_m = 0.5 \text{ V}$ ;  $I_m = 0.8 \text{ A}$ ), it is found:  $R_d = 23.53 \text{ } \Omega$ .

The present work gives, for the first time, an estimation of the dynamic resistance.

This estimation of  $R_d$  at the maximum power point shows that, like  $R_{sh}$ ,  $R_d \gg R_s$ .

Equation (31) shows that the variation  $\Delta I_m$  of the current, due to the introduction of  $R_d$  in the solar cell characteristics, at the maximum power point is:

$$\Delta I_m = \frac{V_m + R_s I_m}{R_d} = 0.024 \text{ A} \quad (32)$$

Hence the relative variation of  $I_m$  is  $\frac{\Delta I_m}{I_m} = 0.03$ . It shows that  $R_d$  leads to a 3% reduction of the current, at the Maximum Power Point (MPP).

It should be noted that  $R_d$  is intensity dependent, as shown by Equations (30) and (31). For the short-circuit ( $V = 0$ ), it is higher, so that its influence on the short-circuit intensity  $I_{sc}$  is very weak. The short-circuit intensity  $I_{sc}$  is linked to the photocurrent,  $I_{ph}$  by the following relation:

$$I_{sc} \approx \frac{I_{ph}}{1 + \frac{R_s}{R_{sh}}} \quad (33)$$

As for the open voltage  $V_{oc}$ , it can be expressed by the semi-empiric relation [21]:

$$V_{oc} \approx V_T \ln \left( \frac{1}{1.5} \frac{J_{ph}}{10^8 \left[ \frac{\text{mA}}{\text{cm}^2} \right]} \right) + \frac{E_g}{q} \quad (34)$$

In Equation (34),  $J_{ph}$  is the photocurrent density,  $E_g$  is the band gap and  $q$  is the electron charge. Hence the introduction of  $R_d$  which leads to a very small decrease of  $I_{sc}$  results in a weak decrease of  $V_{oc}$ . But as shown above, its influence on  $I_m$  at the maximum power point is not negligible. Consequently, the dynamic resistance  $R_d$  has an influence on the maximum output power  $P_m = I_m V_m$ , while its influence on  $I_{sc}$  and  $V_{oc}$  is negligible.

### 4. Conclusion

The capacitance of the solar cell was investigated and its variation with the volt-

age was analyzed. The dynamic resistance  $R_d$ , linked to the parasitic capacitance has been introduced in the dynamic modelling of the solar cell.  $R_d$  has been introduced in the current-voltage characteristics and its value has been estimated at the maximum power point. It has been shown that it has a significant influence on the maximum power current  $I_m$  and consequently on the maximum power  $P_m$ . Hence, the introduction of the dynamic resistance  $R_d$  in the I - V characteristics is quite relevant.

## Conflicts of Interest

The author declares no conflicts of interest regarding the publication of this paper.

## References

- [1] Fezzani, A., Mohamed, I.H., Drid, S., Zaghba, L., Bouchakour, A. and Benbitour, M.K. (2017) Experimental Investigation of Effects of Partial Shading and Faults on Photovoltaic Modules Performances. *Leonardo Electronic Journal of Practices and Technologies*, No. 31, 183-200.
- [2] Izadian, A., Pourtaherian, A. and Motahari, S. (2012) Basic Model and Governing Equation of Solar Cells Used Bin Power Control Applications. 2012 *IEEE Energy Conversion Congress and Exposition*, Raleigh, 15-20 September 2012, 1483-1488. <https://doi.org/10.1109/ECCE.2012.6342639>
- [3] Kebir, S.T. (2020) A Summary of Methods to Get Parameters Values of Photovoltaic Cells/Panels. *Journal of Renewable Energies*, **23**, 20-40.
- [4] Ishaque, K., Salam, Z. and Taheri, H. (2011) Accurate MATLAB Simulink PV System Simulator Based on a Two-Diode Model. *Journal of Power Electronics Korea Science*, **11**, 179-187. <https://doi.org/10.6113/JPE.2011.11.2.179>
- [5] Dhar, S., Sridhar, R. and Avasthy, V. (2012) Modeling and Simulation of Photovoltaic Arrays. <https://www.iitk.ac.in/npsc/Papers/NPSC2012/papers/12118.pdf>
- [6] Ishaque, K., Salam, Z., Taheri, H. and Syafaruddin (2011) Modeling and Simulation of Photovoltaic (PV) System during Partial Shading Based on a Two-Diode Model. *Simulation Modelling Practice and Theory*, **19**, 1613-1625. <https://doi.org/10.1016/j.simpat.2011.04.005>
- [7] Babu, C. and Gurjar, S. (2014) A Novel Simplified Two-Diode Model of Photovoltaic (PV). *IEEE Journal of Photovoltaic*, **4**, 1156-1161. <https://doi.org/10.1109/JPHOTOV.2014.2316371>
- [8] De Rosa, M., Tagliafico, L.A., *et al.* (2015) Dynamic Thermal Model for Hybrid Photovoltaic Panels. *Energy Procedia*, **81**, 345-353. <https://doi.org/10.1016/j.egypro.2015.12.104>
- [9] Zondag, H.A., De Vries, D.W. and Van Halder, W.G.J. (2003) The Yield of Different Combined PV-Thermal Collector Designs. *Solar Energy*, **74**, 253-269. [https://doi.org/10.1016/S0038-092X\(03\)00121-X](https://doi.org/10.1016/S0038-092X(03)00121-X)
- [10] Merhej, P., Dallago, E. and Finarelli, D. (2006) Effect of Capacitance on the Output Characteristics of Solar Cells. <https://www.ims.unipv.it/FIRB2006/pub/Merhej10.pdf>
- [11] Oprea, M.I., Sopataru, S.V., Sera, D., Poulsen, P.B. and Thorsteinsson, S. (2017) Degradation in c-Si PV Panels Using Electrical Impedance Spectroscopy. <https://doi.org/10.1109/PVSC.2016.7749885>
- [12] Kim, K.A., Xu, C.Y., Jin, L. and Krein, P.T. (2013) A Dynamic Photovoltaic Model

- Incorporating Capacitive and Reverse-Bias Characteristics. *IEEE Journal of Photovoltaics*, **3**, 1334-1341. <https://doi.org/10.1109/JPHOTOV.2013.2276483>
- [13] Jumar, R.A., Suresh, M.S. and Nagaraju, J. (2006) Effect of Solar Array Capacitance on the Performance of Switching Shunt Voltage Regulator. *IEEE Transactions on Power Electronics*, **21**, 543-548. <https://doi.org/10.1109/TPEL.2005.869779>
- [14] Mora-Sero, I., Garcia-Belmonte, G., Boix, P.P., Vazquez, M.A. and Bisquert, J. (2009) Impedance Spectroscopy Characterisation of Highly Efficient Silicon Solar Cells under Different Light Illumination Intensities. *Energy & Environmental Science*, **2**, 678. <https://doi.org/10.1039/b812468j>
- [15] Ershov, M., Liu, H.C., Li, L., Buchanan, M., Wasilevski, Z.R. and Jonscher, A.K. (1998) Negative Capacitance Effect in Semiconductor Devices. *IEEE Transactions on Electron Devices*, **45**, 2196-2206. <https://doi.org/10.1109/16.725254>
- [16] Niu, Q., Wetzelaer, A.H., Blom, P.W.M., *et al.* (2018) Origin of Negative Capacitance in Bipolar Organic Diodes. *Physical Review Letters*, **120**, Article ID: 116602. <https://doi.org/10.1103/PhysRevLett.120.116602>
- [17] Guan, M., Niu, L.T., Zhang, Y., Liu, X.F., Li, Y.Y. and Zeng, Y.P. (2017) Space Charges and Negative Capacitance Effect in Organic Light-Emitting Diodes by Transient Current Response Analysis. *RSC Advances*, **7**, 50598-50602. <https://doi.org/10.1039/C7RA07311A>
- [18] Grehant, B. (1990) Cours de Physique des Semiconducteurs. EYROLLES, Paris.
- [19] Sahin, G. (2016) Effect of Wavelength on the Electrical Parameters of a Vertical Parallel Junction Silicon Solar Cell Illuminated by Its Rear Side in Frequency Domain. *Results in Physics*, **6**, 107-111. <https://doi.org/10.1016/j.rinp.2016.02.003>
- [20] Selma, M.S., Diatta, I., Traoré, U., Diouf, M.S., Habiboulahh, L., Wade, M. and Sissoko, G. (2018) Diffusion Capacitance in a Silicon Solar Cell under Frequency Modulated Illumination: Magnetic Field and Temperature Effects. *Journal of Scientific and Engineering Research*, **5**, 317-324.
- [21] Shah, A.V., Platz, R. and Keppner, H. (1995) Thin-Film Silicon Solar Cells: A Review and Selected Trends. *Solar Energy Materials and Solar Cells*, **38**, 501-520. [https://doi.org/10.1016/0927-0248\(94\)00241-X](https://doi.org/10.1016/0927-0248(94)00241-X)